# Design, synthesis and efficacy of novel G protein-coupled receptor kinase 2 inhibitors

**ARTICLE** *in* EUROPEAN JOURNAL OF MEDICINAL CHEMISTRY · SEPTEMBER 2013

Impact Factor: 3.45 · DOI: 10.1016/j.ejmech.2013.08.039 · Source: PubMed

European Journal of Medicinal Chemistry 69 (2013) 384–392

Contents lists available at ScienceDirect

European Journal of Medicinal Chemistry

journal homepage: http://www.elsevier.com/locate/ejmech

Original article

# Design, synthesis and efficacy of novel G protein-coupled receptor kinase 2 inhibitors

Alfonso Carotenuto [a, 1], Ersilia Cipolletta [b, 1], Isabel Gomez-Monterrey [a, 1], Marina Sala [b], Ermelinda Vernieri [b], Antonio Limatola [a], Alessia Bertamino [b], Simona Musella [b], Daniela Sorriento [c], Paolo Grieco [a], Bruno Trimarco [c], Ettore Novellino [a], Guido Iaccarino [d, e, **], Pietro Campiglia [b, *]

[a] Dipartimento di Farmacia, "Federico II" University of Naples, Italy
[b] Dipartimento di Farmacia, University of Salerno, Italy
[c] Dipartimento di Scienze Biomediche Avanzate, "Federico II" University of Naples, Italy
[d] Dipartimento di Medicina e Chirurgia, University of Salerno, Italy
[e] IRCCS, "Multimedica", Milano, Italy

ARTICLE INFO

*Article history:*
Received 8 April 2013
Received in revised form
19 July 2013
Accepted 22 August 2013
Available online 13 September 2013

*Keywords:*
GRK2 inhibitors
Cardiovascular system
Cyclic peptides
NMR conformational analysis

ABSTRACT

G protein-coupled receptor kinase 2 (GRK2) is a relevant signaling node of the cellular transduction network, playing major roles in the physiology of various organs/tissues including the heart and blood vessels. Emerging evidence suggests that GRK2 is up regulated in pathological situations such as heart failure, hypertrophy and hypertension, and its inhibition offers a potential therapeutic solution to these diseases. We explored the GRK2 inhibitory activity of a library of cyclic peptides derived from the HJ loop of G protein-coupled receptor kinases 2 (GRK2). The design of these cyclic compounds was based on the conformation of the HJ loop within the X-ray structure of GRK2. One of these compounds, the cyclic peptide **7**, inhibited potently and selectively the GRK2 activity, being more active than its linear precursor. In a cellular system, this peptide confirms the beneficial signaling properties of a potent GRK2 inhibitor. Preferred conformations of the most potent analog were investigated by NMR spectroscopy.


## 1. Introduction

The G protein-coupled receptor kinase family (GRKs) constitutes a group of seven protein kinases that specifically recognize and phosphorylate agonist-activated G protein coupled receptors (GPCRs) [1]. GRKs-mediated receptor phosphorylation triggers the binding of arrestin proteins that uncouple receptors from G proteins leading to rapid desensitization [2–4]. As a result of β-arrestin binding, phosphorylated receptors are also targeted for clathrin-mediated endocytosis, a process that classically serves to resensitize and recycle receptors back to the plasma membrane [5]. In addition, both arrestins and GRKs participate in signal propagation, cooperating in the assembly of macromolecular complexes in the receptor environment and interacting with different components of signal transduction [1,6]. The seven mammalian GRKs family can be divided into three subfamilies based on sequence and functional similarity: visual GRK subfamily (GRK1 and GRK7), the β-adrenergic receptor kinase (GRK2/GRK3), and the GRK4 subfamily (GRK4, GRK5 and GRK6) [1,7]. All GRKs share a common topological structure that includes an N-terminal regulator of G protein signaling homology domain (RH), a central kinase catalytic domain, and a C-terminal region containing a pleckstrin homology domain (PH) [1,8]. The best-characterized member of this family is the ubiquitously expressed GRK2, also known as β-adrenergic receptor kinase 1 (β-ARK1) [9]. Among others, GRK2 plays a major role in the agonist-specific desensitization of β-adrenergic

*Abbreviations:* DPC, dodecylphosphocholine; SAR, structure–activity relationship; DCM, dichloromethane; DIPEA, *N*,*N*-diisopropylethyl-amine; DMF, *N*,*N*-dimethylformamide; $Pr_3SiH$ or TIS, triisopropylsilane; TFA, trifluoroacetic acid; Fmoc, 9-fluorenyl-methoxycarbonyl; HOBt, *N*-hydroxy-benzotriazole; HBTU, 2-(1*H*-benzotriazole-1-yl)-1,1,3,3-tetramethyluronium hexafluoro-phosphate; Trt, trityl; Pbf, 2,2,4,6,7–pentamethyldihydro benzofuran-5-sulfonyl; RP-HPLC, reversed-phase high performance liquid chromatography; ESI, electrospray ionization; LCQ, liquid chromatography quadrupole mass spectrometry; ATP, adenosine triphosphate; EDTA, Ethylene diamine tetraacetic acid; EGTA, ethylene glycol tetraacetic acid; cAMP, cyclic adenosine monophosphate.

* Corresponding author. Pharmaceutical Science, University of Salerno, Salerno, Italy. Tel.: +39 089 969242.
** Corresponding author. Department of Medicine and Surgery, University of Salerno, Salerno, Italy. Tel.: +39 089 965021.
*E-mail addresses:* giaccarino@unisa.it (G. Iaccarino), pcampigl@unisa.it (P. Campiglia).
[1] These authors contributed equally to the work.

0223-5234/$ – see front matter © 2013 Published by Elsevier Masson SAS.
http://dx.doi.org/10.1016/j.ejmech.2013.08.039

**Table 1**
Different peptide fragments considered in this study.

| Name | | Sequences | | | | | | | |
|---|---|---|---|---|---|---|---|---|---|
| KRX-$683_{107}$ | Myristyl | G | L | L | R | r | H | S | |
| KRX-$683_{124}$ | Lauryl | G | L | L | R | r | H | S | I |
| $^{383-390}$HJ loop (**1**) | | K | L | L | R | G | H | S | P |
| **2** | | G | L | L | R | r | H | S | |
| **3** | | G | L | L | R | r | H | S | I |

receptors (βAR), and therefore in the signal transduction pathway of physiological relevance in the cardiovascular system [9–11]. Alterations in GRK2 levels and/or activity may have important effects in several cardiovascular pathologies, such as myocardiac ischemia, hypertrophy, and hypertension, in which it is up regulated [12–15]. In heart failure (HF), the relationship with increased cardiac GRK2 protein levels has been established in animal models and in patients [16–20]. These data underline the importance of GRK2 levels as a marker of predisposition to cardiac dysfunction [21,22] and support the idea that GRK2 offers a potential therapeutic target [9,23,24]. In fact, the inhibition of GRK2 activity by overexpression of GRK2ct (also termed β-ARKct), a construct that inhibits endogenous GRK2, has provided a successful approach for restoring cardiac function in mouse models with heart failure [25]. Nevertheless, β-ARKct failed to deliver to the clinical scenario due to its dimension (≈200 amino acids) and its need of genetic tools to express in the target tissue (adenovirus). Other inhibitors of GRK2 activity are currently available, even if they are characterized by low sensitivity and specificity [26–29]. Strategies to selectively inhibit the GRK2 activity have been attempted using shorter peptides [30–32] or RNA aptamers [33]. Myristyl or lauryl glycine derivatives of short peptides, such as KRX-$683_{107}$ and KRX-$683_{124}$ (Table 1), proved to be potent inhibitors of the kinase and possess hypoglycemic effect in animal models of Type 2 diabetes [32], and insulin resistance [34]. The peptide fragments of these compounds closely resemble the catalytic fragment 383–390 KLLRGHSP of GRK2 (**1**). This fragment is composed by the last part of the α-helix F (residues 383–386) and the first part of a strand (residues 387–390, Table 1) within the HJ loop. Several crystallographic and mutational studies, have pointed to HJ-αG residues as being involved in substrate binding and in binding to upstream activators [30,31]. We have recently found that peptides **2** and **3**, which are the not acylated derivatives of KRX-$683_{107}$ and KRX-$683_{124}$, respectively (Table 1), selectively inhibit GRK2 *in vitro* [35]. Hence, these compounds are valuable starting points for the development of novel GRK2 inhibitors. Furthermore, conformational analysis of these peptides clearly indicated that their structures are very similar to the X-ray structure of the fragment encompassing the HJ loop of the GRK2 [36], indicating that the isolated peptide could keep the 3D structure of the protein segment.

**Table 2**
Structure, inhibition activities, and analytical data of peptides **2**–**9**.

| Com. | Sequence | Inhibition[a] | | HPLC[c] | ESI-MS (M + H) | |
|---|---|---|---|---|---|---|
| | | GRK2[b] | GRK5[b] | *k′* | Calcd | Found |
| **2**[d] | GLLRrHS | 47.6 ± 5.5 | <5 | 1.70 | 836.97 | 837.66 |
| **3**[d] | GLLRrHSI | 49.6 ± 6.3 | <5 | 1.72 | 950.13 | 950.70 |
| **4** | [GLLRrHS] | 47.8 ± 6.0 | <5 | 1.70 | 819.96 | 820.53 |
| **5** | [GLLRrHSI] | 37.2 ± 10.7 | <5 | 1.85 | 933.12 | 933.80 |
| **6** | [KLLRrHD] | 36.3 ± 4.4 | <5 | 1.72 | 919.09 | 920.13 |
| **7** | [KLLRrHD]I | 55.3 ± 4.6 | <5 | 1.75 | 1032.25 | 1033.11 |
| **8** | [KLLRGHD] | 47.2 ± 4.5 | <5 | 1.76 | 819.47 | 820.51 |
| **9** | [KLLRGHD]I | 33.7 ± 7.8 | <5 | 1.78 | 933.12 | 933.68 |

[a] Data represent mean values (±SD) of three independent determinations.
[b] GRK2 and GRK5 purified proteins activity (50 ng) were tested on rod outer segments (ROS) in presence or absence of 1 μM inhibitors.
[c] *k′* = [(peptide retention time solvent retention time)/solvent retention time].
[d] Already reported in Ref. [34].

Based on these results, we designed, synthesized, and evaluated the GRK2 inhibitor activities of small libraries of cyclic peptides. In addition, we discussed the biological effects of GRK2 inhibition on beta adrenergic receptor signaling for the most potent derivative characterized in this work.

## 2. Results

### 2.1. Design

We have recently found that peptides **2** and **3** selectively inhibit GRK2 *in vitro*. Their NMR solution conformations are very similar to the crystal structure of the fragment encompassing the HJ loop of the GRK2 (pdb entry 3CIK, Fig. 1) [35,36]. Hence, it can be hypothesized that the active conformation of the peptides resembles the HJ loop crystal structure. Accordingly, the stabilization of the peptide 3D structure by, for example, the cyclization of these linear compounds can be considered as a valid approach to the identification of more potent (stable and selective) compounds. As evident from Fig. 1, N- and C-terminal sides of the loop fragment are relatively close (~5 Å), hence we first carried out a head-to-tail cyclization of peptides **2** and **3** leading to peptides **4** and **5**, respectively (Table 2). The design of a second group of cyclic peptides is based on the consideration that, in the GRK2 crystal structure, the amino

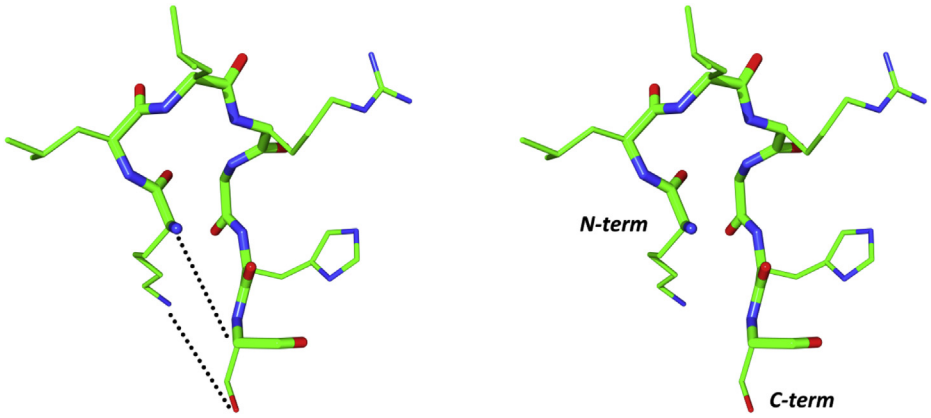


**Fig. 1.** Stereoview of the crystal structure of the fragment 383–390 of GRK2 (**1**, pdb entry 3CIK). Heavy atoms are shown with different colors (carbon, green; nitrogen, blue; oxygen, red). Hydrogen atoms are not shown for clarity. Cyclization strategies are shown as dotted lines. (For interpretation of the references to color in this figure legend, the reader is referred to the web version of this article.)

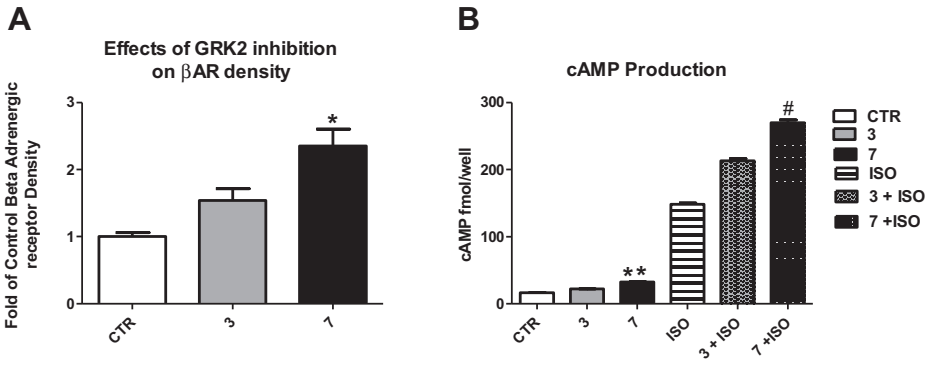


**Fig. 2.** (A) $\beta_2$-adrenergic receptors density in HEK-293 cells treated with peptides **3** and **7** (1 μM for 1 h). Each data point represents the mean ± SEM of 3 independent experiments; * $p$-value ≤0.05. (B) cAMP production in HEK-293 cells treated with **3** and **7** as determined by cAMP immunoassay. ISO: Isoproterenol, 0.1 μM. Each data point represents the mean ± SEM of 3 independent experiments; $^{**}p < 0.0001$ vs Ctr; $^{\#}p < 0.01$ vs ISO.

group of K383 side chain points towards the Ser389 side chain (Fig. 1). Hence, the stabilization of the peptide structure was also sought through a side chain-to-side chain cyclization approach. The cyclic peptides **6** and **7** (Table 2) were synthesized from linear peptides which contain the original residue Lys383 of GRK2 instead of Gly1 and an Asp residue in place of Ser7 residue. These two residues are linked by a side chain amide bond. For comparative purpose the analogs **8** and **9**, containing the original Gly387 residue at the position 5, were also synthesized and tested for their activity to inhibit GRK2.

### 2.2. Synthesis

Head-to-tail cyclic peptides (**4** and **5**) were prepared on acid-labile 2Cl-Trt resin by solid-phase synthesis of linear peptide sequences, using the Fmoc protection strategy, followed by cyclization and side-chain deprotection in solution [37,38]. The preparation of cyclic peptides, **6**–**9**, through a side-chain-to-side-chain cyclization, was carried out after removal of the Allyl/Alloc protection according to strategy reported by Grieco et al. [39]. Peptide analytical data are reported in Table 2.

### 2.3. Biological activity

The effectiveness of these peptidesto inhibit the GRK2 kinase activity was assessed by *in vitro* rhodopsin phosphorylation assay and visualized by autoradiography of dried gels (See Fig. 1 in Supporting information). Peptides with cyclic modifications retain the ability to inhibit GRK2, although in some cases (such as peptides **5**, **6** and **9**) they lose some efficacy compared to the original peptides (Table 2). In particular, C-terminal Ile residue caused different effects depending on the peptide structure. In fact, in linear peptides the inhibitory activity was not affected by the C-terminal Ile (peptide **2** vs. peptide **3**). In cyclic peptides, C-terminal Ile can both increase (peptide **6** vs. peptide **7**) and decrease (peptide **4** vs. peptide **5** and peptide **8** vs. peptide **9**) the inhibitory activity. Overall, lactam cyclic peptide **7** is the most active to inhibit GRK2 gaining about 10% of activity compared to the parent peptide **3**.

In addition, the dose response curves for the most potent compounds **3** and **7**, at concentration range from $10^{-3}$ to $10^{-9}$ M, confirm the ability of these compounds to inhibit GRK2-mediated ROS phosphorylation in dose-dependent manner (see Supporting information Fig. S2). Calculated $IC_{50}$'s were $3.4 \pm 0.3 \cdot 10^{-7}$ M (peptide **3**) and $1.2 \pm 0.6 \cdot 10^{-7}$ M (peptide **7**) confirming a slightly higher potency of the latter.

Next, to verify whether these peptides selectively inhibit GRK2, we repeated the activity assay substituting GRK5 to GRK2 purified protein (Table 2). GRK2 selective inhibition is suggested by the evidence that all peptides don't affect GRK5 kinase activity on rhodopsin phosphorylation levels.

To confirm the effectiveness of GRK2 inhibition in a cellular setup, we tested the effects of GRK2 inhibitors in cells on beta adrenergic receptors density in HEK-293 cells stably over-expressing the $\beta_2$ adrenergic receptor ($\beta_2$AR) [34]. In HEK-293 cells, incubation with compound **3** or the cyclic peptide **7** (1 μM) results in the increase in $\beta_2$AR density, consistent with an effective inhibition of GRK2 (Fig. 2A). Accordingly, basal and βAR stimulated cAMP production in HEK-293 cells was significantly affected by peptide **7** (Fig. 2B). Interestingly, peptide **7** results to be more effective than the lead compound **3** in both assays.

Previous experiments on intact cells indicate that peptides **3** and **7** are able to penetrate cell membrane. To demonstrate this point, we measured the internalization of both fluorescently labeled peptides (**Fl-3** and **Fl-7**, respectively). As observed in Fig. 3A and B, both peptides are able to cross cell membrane with the linear compound **Fl-3** incorporated to cells more effectively than compound **Fl-7**.

### 2.4. NMR analysis of cyclic peptide 7

NMR analysis of peptide **7** was performed in water and DPC[2] micelle solutions. Almost complete $^1$H NMR chemical shift assignments (Supporting information, Tables S1–S2) were achieved according to the Wüthrich procedure [40] via the usual systematic application of TOCSY, and NOESY experiments in both environments. Considering the spectra in water solution, all NMR parameters indicated structural flexibility (Table S1). For example, no standard α-helix or β-sheet structure from $H_\alpha$ CSI (chemical shift index) values [41], and no unambiguous medium- or long-range backbone NOE connectivities were found in the NOESY spectrum of the peptides. Only strong $d_{\alpha N}(i, i+1)$ NOEs, which are generally observed in random structures, appeared along the entire length of the peptides. In contrast, several NMR parameters indicate that peptides are better structured in DPC solution and that they share very similar conformations. In particular, $H_\alpha$ resonances (Table S2), and many NOE signals (Table S3, Supporting information) clearly point to a folded structure encompassing the N-terminal residues (1–5) and extended conformation of residues 6–8. Non-trivial medium range NOE interactions, among which $d_{\alpha N}(i, i+2)$ 1–3, 2–4, 3–5, $d_{NN}(i, i+2)$ 2–4, and $d_{\alpha N}(i, i+3)$ 1–4, are observed

[2] Abbreviations used for amino acids and designation of peptides follow the rules of the IUPAC-IUB Commission of Biochemical Nomenclature in J. Biol. Chem. 247 (1972) 977-983. Amino acid symbols denote L-configuration unless indicated otherwise.

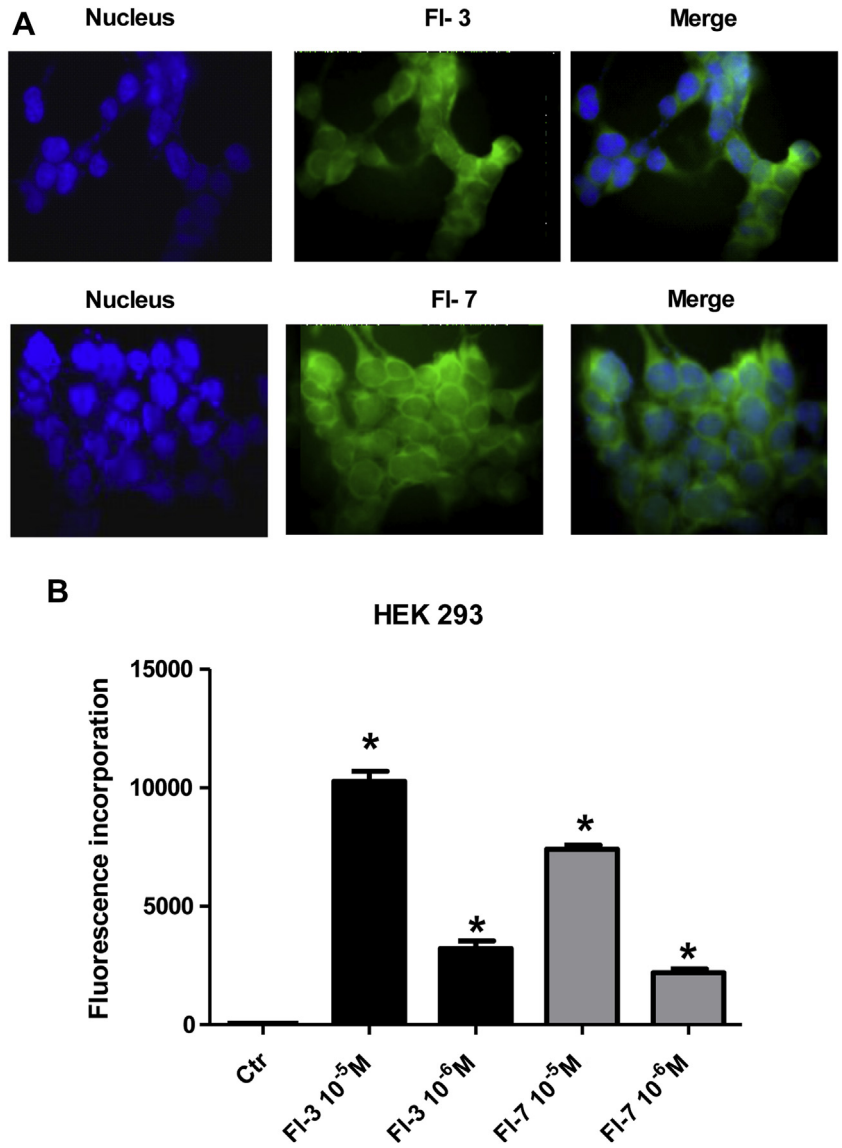


**Fig. 3.** (A) Incorporation of fluorescently labeled peptides into $\beta_2$HEK-293 cells. The cells were incubated with 1 μM **Fl-3** (upper panel) and **Fl-7** (lower panel) for 1 h. Images were obtained by confocal microscopy. (B) Quantification of 3 experiments measuring fluorescence incorporation of the cells incubated with either **Fl-3** or **Fl-7**, at either 10 μM or 1 μM $p < 0.01$ vs Control (Ctr).

pointing to a turn-helical structure along residues 1–5. Low temperature coefficient of the backbone amide proton of residue 4 ($-\Delta\delta/\Delta T \sim 4$ ppb/K) confirms this hypothesis. C-terminal region is in extended conformation as indicated by the strong $d_{\alpha N}(i, i+1)$ NOEs and large $^3J_{\text{HN-H}\alpha}$ coupling constants. Finally, NOE contacts between Arg4 and His6 side chains indicate that these are spatially close.

NOE distance restraints obtained for peptide **7** in DPC micelles were used as the input data for a simulated annealing structure calculation using the program DYANA [42]. Superposition of the 10 lowest energy conformers of **7** is shown in Fig. 4. The mean RMS to the average structure for backbone heavy atoms is 0.20 Å. Since a β-turn may be defined as four consecutive non-helical residues that have a $C_\alpha(i)$-$C_\alpha(i+3)$ distance $< 7$ Å, two β-turns that involve Gly1 to Arg4 and Leu2 to D-Ala5, can be identified.

The first β-turn structure is stabilized by a hydrogen bond between the carbonyl oxygen of Lys1 and the amide hydrogen of Arg4. Residues 6 and 7 are in extended conformations, residue 8 is more flexible. The side chain are also well defined, the RMSD for all heavy atoms is 0.74 Å. The side chains of Arg4 and His6 are close and form a positively charged hydrophilic surface while Leu2 and Leu3 side chains establish a hydrophobic surface pointing in the opposite direction.

## 3. Discussion

The aim of the present study was the design of analogs of peptides **2**, and **3**, potent and selective inhibitors of GRK2 [35]. Peptides **2** and **3** are the not acylated derivatives of compounds KRX-$683_{107}$ and KRX-$683_{124}$, respectively (Table 1), in turn derived from the fragment 383–390 of the HJ loop of GRK2 (**1**, Table 1) [32]. Conformational similarity of these peptide to the protein fragment within the crystal structure of GRK2 [36], prompted us to design novel analogs of peptides **2** and **3** based on head-to-tail and side chain-to-side chain cyclization, according to the HJ loop structure (Fig. 1). Hence, the lactam were introduced as a conformational constraint to stabilize the putative 3D active conformation. The utility of backbone or side chain cyclization has been well

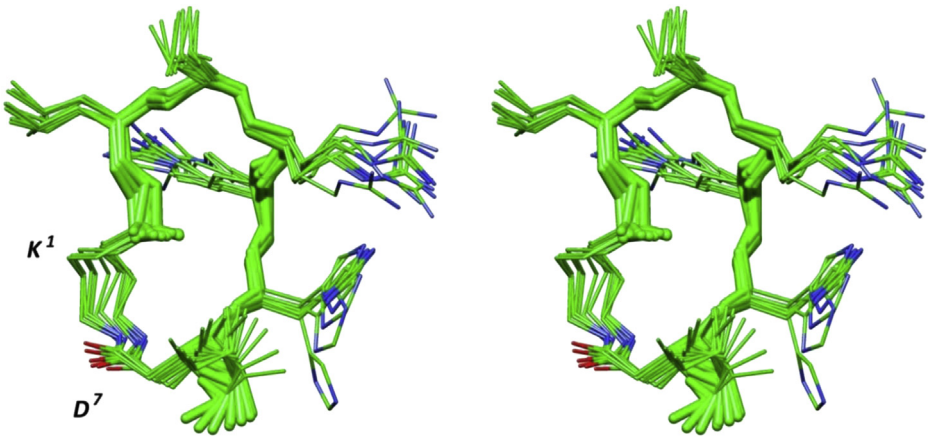


**Fig. 4.** Stereoview of the 10 lowest energy conformers of **7**. Structures were superimposed using the backbone heavy atoms. Heavy atoms are shown with different colors (carbon, green; nitrogen, blue; oxygen, red). Hydrogen atoms are not shown for clarity. (For interpretation of the references to color in this figure legend, the reader is referred to the web version of this article.)

established in peptides, and it has been demonstrated to increase biological activity and selectivity since they are usually more stable in metabolism than the parent linear molecules [43]. In this context, lactam bridges are preferable over disulfide ones due to their chemical stability [44].

All cyclic peptides retain the ability to inhibit GRK2 (Table 2) demonstrating the validity of the design strategy. Potency fluctuations were observed upon the insertion of Ile8 in cyclic analogs. Probably, conformational restraints imposed by the cyclization also affect exocyclic Ile residue spatial orientation which, in turn, influences the inhibitory activity. Cyclic peptide **7** is the most active in the GRK2 inhibition overcoming of about 10% its precursor (peptide **3**). Interestingly, peptides also retain selectivity towards GRK2 since they don't affect GRK5 kinase activity on rhodopsin levels. To bring our observation to a biological setup, we tested the effects of GRK2 inhibitors in cells on the beta adrenergic receptors density. Indeed, it is known that GRK2 inhibition can change the affinity state of the beta adrenergic receptor by preventing desensitization [45], furthermore recent evidences suggest that also the total number of β adrenergic receptors is under the control of GRK2 activity [46], thus indicating that the kinase also control downregulation, the major and most effective mechanism of regulation of βAR signaling. Interestingly, peptide **7** results to be more effective than the lead compound **3** to increase $\beta_2$AR density (Fig. 2A). Similar results are obtained in cAMP production studies. In fact, **7** increases both basal and $\beta_2$AR stimulated cAMP production in cells (Fig. 2B). These results are particularly important since they indicated these peptides are able to penetrate the cell membrane by itself without the need of acylation (as for KRX-$683_{124}$), conjugation with cell penetrating peptides, etc. To confirm this important suggestion, we measured the internalization of both fluorescently labeled peptides (**FI-3** and **FI-7**, respectively). As observed in Fig. 3A and B, both peptides cross cell membrane in an effective manner. Probably, peptide **7** highest potency in the inhibition of GRK2 kinase activity is the predominant factor determining the observed significant increase of $\beta_2$ adrenergic receptor density and cAMP production.

Promising compound **7** was also investigated for its conformational preferences. NMR analysis of peptide **7** was performed in water and DPC micelle solutions. It is well-known that water is the best medium to be used for the structural study of peptides. Unfortunately it favors the prevailing of disordered and flexible conformations so that the building of a 3D model is often precluded. Mixtures made up of water and organic solvents are the most used media to produce environmental constraints. In particular, alcohols and fluoro alcohols are known to stabilize peptide secondary structures [47]. Micelle solutions are membrane mimetic environments and are largely used for conformational studies of peptide hormones and antimicrobial peptides [48]. In this case, a micellar

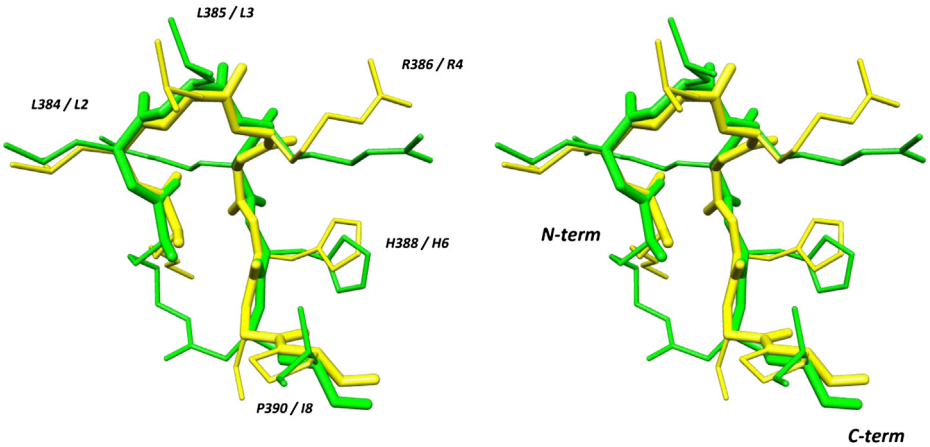


**Fig. 5.** Stereoview of **7** lowest energy conformer (green) and fragment 383–390 of GRK2 (**1**, yellow, pdb entry 3CIK). The structures are superimposed using the backbone heavy atoms. (For interpretation of the references to colour in this figure legend, the reader is referred to the web version of this article.)

solution of DPC was chosen since GRK2 phosphorylation of GPCRs occurs close to the plasma membrane. Peptide **7** structure in DPC micelles is characterized by two $\beta$-turns that involve Gly1 to Arg4 and Leu2 to D-Arg5, followed by a short extended region encompassing residues 6 and 7 (Fig. 5). Compared to the linear parent peptides, compound 7 shows a lower conformational flexibility (in fact, the backbone heavy atoms RMSD decreases from 0.31 to 0.20 Å, compared to the linear analog) [35].

More interestingly, the NMR structures of peptide **7** are very similar to the crystal structure of the fragment encompassing the HJ loop of the GRK2 (pdb entry 3CIK) [36]. Fig. 5 shows the superposition of the NMR structure of **7** with that of the fragment 383–390 of the GRK2. Equivalent backbone atoms of **7** and GRK2 superimpose to an RMSD of 0.17 Å. It can be also observed the good overlapping of the unchanged side chains which occupies similar space regions. Also, Ile8 side chain is well overlapped with that of Pro390, supporting the positive contribution of this residue on peptide activity. Therefore, the isolated peptide keeps the 3D structure of the protein segment and likely competes with the activation functions of this loop [30,31].

## 4. Conclusion

GRK2 is involved in the regulation of many pivotal cell functions, and is therefore a key player in human health and disease, such as in determinate pathological cardiovascular processes as heart failure. Hence, modulation of its activity could be exploited with therapeutic purposes. The present study describes the design, synthesis, and biological evaluation of a series of cyclic peptides which are able to selectively inhibit GRK2. In particular, cyclic peptide **7** demonstrated to increase the inhibitory potency of the linear parent **3**. Our results showed that **7** also increased, more effectively than **3**, the density of β adrenergic receptors and the βAR stimulated cAMP production in cardiac cells, further confirming the GRK2 control on regulation of βAR signaling. These findings confirm that conformational-based chemical modification of the linear fragment encompassing the HJ loop of the GRK2 is an effective approach to identify structures able to modulate GRK2 activity through inhibition. Further *in vivo* experiments aimed to verify the potentiality of this peptide in the cardiovascular system as well as the preparation of novel more potent and selective peptide and peptidomimetic derivatives are in progress.

## 5. Experimental section

### 5.1. Synthesis

The synthesis of GRK2 analogs was performed according to the solid phase approach using standard Fmoc methodology in a manual reaction vessel [37]. $N^{\alpha}$-Fmoc-protected amino acids, Rinkamide-resin, HOBt, HBTU, DIEA, Piperidine and Trifluoroacetic acid were purchased from Iris Biotech (Germany). Peptide synthesis solvents, reagents, as well as $CH_3CN$ for HPLC were reagent grade and were acquired from commercial sources and used without further purification unless otherwise noted. The first amino acid, $N^{\alpha}$Fmoc-Xaa-OH (Xaa = Ile, Ser($^t$Bu), Asp($^t$Bu)), was linked on to the Rink resin (100–200 mesh, 1% DVB, 0.75 mmol/g) previously deprotected by a 25% piperidine solution in DMF for 30 min.

The following protected amino acids were then added stepwise: $N^{\alpha}$-Fmoc-His($N_{(im)}$trityl(Trt))-OH, $N^{\alpha}$-Fmoc-DArg(Pbf)-OH (or $N^{\alpha}$-Fmoc-DAla-OH) $N^{\alpha}$-Fmoc-Arg(Pbf)-OH, $N^{\alpha}$-Fmoc-Leu-OH, $N^{\alpha}$-Fmoc-Gly-OH. Each coupling reaction was accomplished using a 3-fold excess of amino acid with HBTU and HOBt in the presence of DIPEA (6 equiv). The $N^{\alpha}$-Fmoc protecting groups were removed by treating the protected peptide resin with a 25% solution of piperidine in DMF (1 × 5 min and 1 × 25 min). The peptide resin was washed three times with DMF, and the next coupling step was initiated in a stepwise manner. The peptide resin was washed with DCM (3×), DMF (3×), and DCM (3×), and the deprotection protocol was repeated after each coupling step.

In addition, after each step of deprotection and after each coupling step, Kaiser test was performed to confirm the complete removal of the Fmoc protecting group, respectively, and to verify that complete coupling has occurred on all the free amines on the resin.

The N-terminal Fmoc group was removed as described above, and the peptide was released from the resin with TFA/$^i$Pr$_3$SiH/$H_2O$ (90:5:5) for 3 h. The resin was removed by filtration, and the crude peptide was recovered by precipitation with cold anhydrous ethyl ether to give a white powder and then lyophilized.

### 5.2. Synthesis of head-to-tail cyclic peptides (*4* and *5*)

The title peptides were synthesized using a 2-chlorotrityl chloride resin. The first $N^{\alpha}$-Fmoc amino acid (0.6–1.2 equiv relative to the resin for 2-chlorotrityl resin) and DIPEA (4 equiv relative to amino acid) were dissolved in dry dichloromethane (DCM) (approx. 10 mL per gram of resin) containing, if necessary, a small amount of dry DMF (enough to facilitate dissolution of the acid). This was added to the resin and stirred for 30–120 min. After stirring, the resin was washed with 3× DCM/MeOH/DIPEA (17:2:1), 3× DCM, 2× DMF and 2× DCM. Other $N^{\alpha}$-Fmoc amino acids (4 equiv) were sequentially coupled as previously described. The final cleavage with AcOH/MeOH/DCM (1:1:8) resulted in protected peptides [38].

#### 5.2.1. General procedure for cyclization

A solution of the linear protected peptide (0.03 mmol) in DMF (6.5 mL) was added at room temperature to a reaction flask containing a solution of *N*-hydroxybenzotriazole (HOBt) (3 equiv, 12 mg, 0.09 mmol), HBTU (3 equiv, 34 mg, 0.09 mmol) and DIPEA (5 equiv, 0.26 mL, 1.5 mmol) in DMF (1 mL). The mixture was stirred for 24 h at room temperature and monitored by TLC. The mixture was concentrated under reduced pressure, and the residue was dissolved in ethyl acetate (AcOEt). The organic phase was washed twice with 5% aqueous sodium bicarbonate ($NaHCO_3$), dried over sodium sulfate ($Na_2SO_4$), and filtered. The solvent was removed by reduced pressure to give the final crude protected peptide.

### 5.3. Synthesis of lactam analogs (*6*, *7*, *8*, and *9*)

The corresponding linear peptides were synthetized as described above and the amino acids $N^{\alpha}$-Fmoc-Asp(Allyl)-OH and $N^{\alpha}$-Fmoc-Lys(Alloc)-OH were used as lactam precursors [39]. After linear assembly, the Nγ-Alloc and the Allyl groups were removed according to the following procedure: 200 mg of peptide resin was washed with dichloromethane (DCM) under Ar and a solution of $PhSiH_3$ (24 equiv) in 2 mL of DCM was added. Subsequently a solution of $Pd(PPh_3)_4$ (0.25 equiv) in 6 mL of DCM was added and the reaction was allowed to proceed under Ar for 30 min. The peptide resin was washed with DCM (3×), DMF (3×) and DCM (4×), and the deprotection protocol was repeated (3×). The macrocyclic lactam ring formation was mediated by addition of HBTU (6 equiv), HOBt (6 equiv) and DIPEA (12 equiv) for 2 h [39]. The process was repeated if necessary (Kaiser test used to monitor completion). The N-terminal Fmoc group was removed and the peptide was released from the resin as described above.

### 5.4. Side-chain deprotection

The protected cyclopeptide (0.02 mmol) was treated with 10 mL of a solution of TFA/triisopropylsilane (TIS)/$H_2O$ 95:2.5:2.5 at room temperature. After 24 h, the reaction mixture was evaporated in

vacuo, and the residue was washed with diethyl ether ($Et_2O$) and concentrated in vacuo, yielding the side chain-deprotected cyclopeptide as a trifluoroacetate salt (quant.).

### 5.5. Synthesis of labeled peptides (**Fl-3**, **Fl-7**)

The starting peptides **3** and **7** were synthesized as described above. Then Fmoc-deprotected, resin-bound peptides, were reacted with 3 equiv of 5(6)-carboxyfluorescein, *N*,*N*′-diisopropyl carbodiimide, and 1-hydroxybenzotriazol, each in DMF for 16 h in 10-mL syringes on a shaker at RT. Reactions were stopped by washing the resins three times each with DMF, methanol, dichloromethane, and diethyl ether. Completeness of N-terminal acylation was confirmed using the Kaiser test.

### 5.6. Purification and characterization

All crude peptides were purified by RP-HPLC on a semi-preparative C18-bonded silica column (Phenomenex, Jupiter, 250 × 10 mm) using a Shimadzu SPD 10A UV/VIS detector, with detection at 210 and 254 nm. The column was perfused at a flow rate of 3 ml/min with solvent A (10%, v/v, water in 0.1% aqueous TFA), and a linear gradient from 10 to 90% of solvent B (80%, v/v, acetonitrile in 0.1% aqueous TFA) over 40 min was adopted for peptide elution. Analytical purity and retention time ($t_R$, Table 2) of each peptide were determined using HPLC conditions in the above solvent system (solvents A and B) programmed at a flow rate of 1 mL/min using a linear gradient from 10 to 90% B over 25 min, fitted with C-18 column Phenomenex, Juppiter C-18 column (250 × 4.60 mm; 5 μ).

All analogs showed >97% purity when monitored at 215 nm. Homogeneous fractions, as established using analytical HPLC, were pooled and lyophilized.

Peptides molecular weights were determined by ESI mass spectrometry. ESI-MS analysis in positive ion mode, were made using a Finnigan LCQ ion trap instrument, manufactured by Thermo Finnigan (San Jose, CA, USA), equipped with the Excalibur software for processing the data acquired. The sample was dissolved in a mixture of water and methanol (50/50) and injected directly into the electrospray source, using a syringe pump, which maintains constant flow at 5 μl/min. The temperature of the capillary was set at 220 °C.

### 5.7. NMR spectroscopy

The samples for NMR spectroscopy were prepared by dissolving the appropriate amount of peptide to obtain a concentration 1–2 mM in 0.55 mL of $^1H_2O$ (pH 5.5), 0.05 mL of $^2H_2O$ for water samples, 200 mM DPC-$d_{38}$ for micelle samples. NMR spectra were recorded on a Varian INOVA 700 MHz spectrometer equipped with a *z*-gradient 5 mm triple-resonance probe head. All the spectra were recorded at a temperature of 25 °C. The spectra were calibrated relative to TSP (0.00 ppm) as internal standard. One-dimensional (1D) NMR spectra were recorded in the Fourier mode with quadrature detection. Water suppression was achieved by using the double-pulsed field gradient spin-echo (DPFGSE) scheme [49]. 2D DQF-COSY [50], TOCSY [51], and NOESY [52] spectra were recorded in the phase-sensitive mode using the method of States [53]. Data block sizes were 2048 addresses in $t_2$ and 512 equidistant $t_1$ values. Before Fourier transformation, the time domain data matrices were multiplied by shifted $\sin^2$ functions in both dimensions. A mixing time of 70 ms was used for the TOCSY experiments. NOESY experiments were run with mixing times in the range of 100–200 ms. The qualitative and quantitative analyses of DQF-COSY, TOCSY, and NOESY spectra, were obtained using the interactive program package XEASY [54]. $^3J_{HN\text{-}H\alpha}$ coupling constants were obtained from 1D $^1H$ NMR and 2D DQF-COSY spectra. Many $^3J_{HN\text{-}H\alpha}$ coupling constants were difficult to measure in DPC solution probably because of a combination of small coupling constants and broad lines. The temperature coefficients of the amide proton chemical shifts were calculated from 1D $^1H$ NMR and 2D TOCSY experiments performed at different temperatures by means of linear regression.

### 5.8. Structural determinations

The NOE-based distance restraints were obtained from NOESY spectra collected with a mixing time of 200 ms. The NOE cross peaks were integrated with the XEASY program and were converted into upper distance bounds using the CALIBA program incorporated into the program package DYANA [42]. Cross peaks which overlapped more than 50% were treated as weak restraints in the DYANA calculation. For each examined peptide, an ensemble of 100 structures was generated with the simulated annealing of the program DYANA. An error-tolerant target function (tf-type = 3) was used to account for the peptide intrinsic flexibility of the peptide. The annealing procedure produced 100 conformations from which 20 structures were chosen, whose interprotonic distances best fitted NOE derived distances, and then refined through successive steps of restrained and unrestrained EM calculations using the Discover algorithm (Accelrys, San Diego, CA) and the consistent valence force field (CVFF) as previously described [55]. Graphical representation was carried out with the UCSF Chimera package [56]. RMS deviation analysis between energy minimized structures were carried out with the program MOLMOL [57].

## 6. *In vitro* methods

### 6.1. GRK activity in rhodopsin phosphorylation assays

To evaluate the effect of all synthesized peptides on GRK2 activity we assessed GRK2 or GRK5 purified proteins by light-dependent phosphorylation of rhodopsin-enriched rod outer segment membranes (ROS) using [γ-$^{32}$P]-ATP as previously described [58]. Briefly, 50 ng of active GRK2 or GRK5 were incubated with ROS membranes in presence or absence of inhibitor peptides in reaction buffer (25 μl) containing 10 mM $MgCl_2$, 20 mM Tris–Cl, 2 mM EDTA, 5 mM EGTA, and 0.1 mM ATP and 10 μCi of [$^{32}$P]γ-ATP. After incubation with white light for 15 min at room temperature, the reaction was quenched with ice-cold lysis buffer and centrifuged for 15 min at 13000*g*. The pelleted material was resuspended in 35 μL protein gel loading dye, electrophoresed and resolved on SDSPAGE 4–12% gradient (Invitrogen), stained with Coomassie blue, destained, vacuum dried, and exposed for autoradiography. Phosphorylated rhodopsin was visualized by autoradiography of dried gels and quantified using a PhosphorImager (Molecular Dynamics). Alternatively, the ROS pellet was washed twice in ice-cold lysis buffer to remove the unbound [γ$^{32}$P]-ATP and then resuspended in 100 μL of buffer and the level of [γ$^{32}$P]-ATP incorporation into ROS was determined by liquid scintillation counter.

### 6.2. β-Adrenoreceptor radioligand binding

Cultured Hembriogenic Kidney cells overexpressing $\beta_2$ adrenergic receptor ($\beta_2$HEK-293) were treated with peptides **3** and **7** 1 μM for one hour. Membrane fraction was prepared by homogenization of whole cell in ice-cold buffer (25 mM Tris–HCl (pH 7.5), 5 mM EDTA, 5 mM EGTA, 1 mM phenylmethylsulfonyl fluoride, 2 μg/ml each leupeptin and aprotinin) as previously described [34].

Total βAR density was determined by incubating 60 μg of sarcolemmal membranes with a saturating concentration of [$^{125}$I]cyanopindolol and 20 μmol/L alprenolol to define nonspecific binding. Assays were conducted at 37 °C for 60 min and then filtered over GF/C glass fiber filters (Whatman) that were washed and counted in a gamma counter [45]. All values are presented as mean ± SEM of three independent experiments. One-way ANOVA was performed to compare the different groups. A significance level of $P < 0.05$ was assumed for all statistical evaluations. Statistics were computed with GraphPad Prism Software (GraphPad Software Inc., version 4, San Diego, CA, USA).

### 6.3. cAMP synthesis

$\beta_2$HEK293 were plated in 96-well plates (10,000 cells/well) and serum starved overnight. Cells were incubated in a fresh medium in the presence **3** and **7** peptides 1 μM for one hour and then stimulated with β adrenergic receptor agonist Isoproterenol 0.1 μM for 15 min. The cAMP quantification was evaluated by enzyme immunoassay, using an EIA commercial kit (RPN 2255 GE Healthcare Bio-Sciences AB, Uppsala, Sweden). The cAMP content present in HEK-293 cell was expressed in fmoles per well. All values are presented as mean ± SEM of three independent experiments. One-way ANOVA was performed to compare the different groups. A significance level of $P < 0.05$ was assumed for all statistical evaluations. Statistics were computed with GraphPad Prism Software (GraphPad Software Inc., version 4, San Diego, CA, USA).

### 6.4. Internalization studies

$\beta_2$HEK-293 overexpressing human $\beta_2$AR cells were plated in 4-well ibidi plate (10,000 cells/well) and serum starved overnight. The cells were then incubated with fluorescently labeled peptides (**Fl-3** and **Fl-7**) 1 μM for 60 min at 37 °C. After washing twice with PBS cell images were taken by using an Eclipse E1000 Fluorescence Microscope (Nikon) and acquired by using Sigma Scan Pro software (Jandel). Images were optimized for contrast in Adobe Photoshop, but no further manipulations were made.

Alternatively HEK-293 cells were plated in 24-well plates (20,000 cells/well) and serum starved overnight The cells were then incubated with fluorescently labeled peptides (**Fl-3** and **Fl-7**) at the concentration of 10 and 1 μM for 60 min at 37 °C. The fluorescence incorporation was quantified on a Tecan Genios plate reader with a 485 nm excitation filter and a 510 nm emission filter using a gain setting of 1.0. The background signal from cells untracted was subtracted. All values are presented as mean ± SEM of three independent experiments. One-way ANOVA was performed to compare the different groups. A significance level of $P < 0.05$ was assumed for all statistical evaluations. Statistics were computed with GraphPad Prism Software (GraphPad Software Inc., version 4, San Diego, CA, USA).

## Acknowledgment

The LC-MS and NMR spectral data were provided by Servizio Interdipartimentale di Analisi Strumentale (CSIAS), Università degli Studi di Napoli "Federico II". The assistance of the staff is gratefully appreciated. This work was supported by a grant from the Italian Ministry of Education (MIUR) (PRIN n° 2009EL5WBP).

## Appendix A. Supplementary data

Supplementary data related to this article can be found at http://dx.doi.org/10.1016/j.ejmech.2013.08.039.

## References

[1] J.A. Pitcher, N.J. Freedman, R.J. Lefkowitz, G protein-coupled receptor kinases, Annu. Rev. Biochem. 67 (1998) 653–692.
[2] S. Ferguson, Evolving concepts in G protein-coupled receptor endocytosis: the role in receptor desensitization and signalling, Pharmacol. Rev. 53 (2001) 1–24.
[3] E. Reiter, R.J. Lefkowitz, GRKs and beta-arrestins: roles in receptor silencing, trafficking and signalling, Trends Endocrinol. Metab. 17 (2006) 159–165.
[4] C.A. Moore, S.K. Milano, J. Benovic. L, Regulation of receptor trafficking by GRKs and arrestins, Annu. Rev. Physiol. 69 (2007) 451–482.
[5] C. Ribas, P. Penela, C. Murga, A. Salcedo, C. Garcia-Hoz, M. Juradopueyo, I. Aymerich, F. Mayor Jr., The G protein-coupled receptor kinase (GRK) interactome: role of GRKs in GPCR regulation and signaling, Biochim. Biophys. Acta 1768 (2007) 913–922.
[6] (a) R.J. Lefkowitz, S.K. Shenoy, Transduction of receptor signals by beta-arrestins, Science 308 (2005) 512–517;
(b) C.J. Hupfeld, J.M. Olefsky, Regulation of receptor tyrosine kinase signaling by GRKs and beta-arrestins, Annu. Rev. Physiol. 69 (2007) 561–577.
[7] (a) M. Oppermann, M. Diverse-Pierluissi, M.H. Drazner, S.L. Dyer, N.J. Freedman, K.C. Peppel, R.J. Lefkowitz, Monoclonal antibodies reveal receptor specificity among G-protein coupled receptor kinases, Proc. Natl. Acad. Sci. U. S. A. 93 (1996) 7649–7654;
(b) J.M. Willets, R.A.J. Challiss, S.R. Nahorski, Non-visual GRKs: are we seeing the whole picture? Trends Pharmacol. Sci. 24 (2003) 626–633.
[8] J. Inglesef, N.J. Freedman, W.J. Koch, R.J. Lefkowit, Structure and mechanism of the G protein-coupled receptor kinases, J. Biol. Chem. 268 (1993) 23735–23738.
[9] P. Penela, C. Murga, C. Ribas, V. Lafarga, F. Mayor Jr., The complex G protein-coupled receptor kinase 2 (GRK2) interactome unveils new physiopathological targets, Br. J. Pharmacol. 160 (2010) 821–832.
[10] T. Evron, T.L. Daigle, M.G. Caron, GRK2: multiple roles beyond G protein-coupled receptor desensitization, Trends Pharmacol. Sci. 33 (2012) 154–164.
[11] P. Penela, C. Murga, C. Ribas, A.S. Tutor, S.F. Peregrin, F.J. Mayor, Mechanisms of regulation of G protein-coupled receptor kinases (GRKs) and cardiovascular disease, Cardiovasc. Res. 69 (2006) 46–56.
[12] N. Dzimiri, P. Muiya, E. Andres, Z. Al-Halees, Differential functional expression of human myocardial G protein receptor kinases in left ventricular cardiac diseases, Eur. J. Pharmacol. 489 (2004) 167–177.
[13] M. Ungerer, K. Kessebohm, K. Kronsbein, M.J. Lohse, G. Richardt, Activation of beta-adrenergic receptor kinase during myocardial ischemia, Circ. Res. 79 (1996) 455–460.
[14] D.J. Choi, W.J. Koch, J.J. Hunter, H.A. Rockman, Mechanism of beta-adrenergic receptor desensitization in cardiac hypertrophy is increased beta-adrenergic receptor kinase, J. Biol. Chem. 272 (1997) 17223–17229.
[15] R. Gros, J.L. Benovic, C.M. Tan, R.D. Feldman, Gprotein- coupled receptor kinase activity is increased in hypertension, J. Clin. Invest 99 (1997) 2087–2093.
[16] J. Theilade, C. Strom, T. Christiansen, S. Haunso, S.P. Sheikh, Differential G protein receptor kinase 2 expression in compensated hypertrophy and heart failure after myocardial infarction in the rat, Basic Res. Cardiol. 98 (2003) 97–103.
[17] C.A. Harris, T.T. Chuang, C.A. Scorer, Expression of GRK2 is increased in the left ventricles of cardiomyopathic hamsters, Basic Res. Cardiol. 96 (2001) 364–368.
[18] X.P. Yi, A.M. Gerdes, F. Li, Myocyte redistribution of GRK2 and GRK5 in hypertensive, heart failure-prone rats, Hypertension 39 (2002) 1058–1063.
[19] K.M. Anderson, A.D. Eckhart, R.N. Willette, W.J. Koch, The myocardial beta-adrenergic system in spontaneously hypertensive heart failure (SHHF) rats, Hypertension 33 (1999) 402–407.
[20] G. Iaccarino, E. Barbato, E. Cipolletta, V. De Amicis, K.B. Margulies, D. Leosco, B. Trimarco, W.J. Koch, Elevated myocardial and lymphocyte GRK2 expression and activity in human heart failure, Eur. Heart J. 26 (2005) 1752–1758.
[21] J.A. Hata, M.L. Williams, J.N. Schroder, B. Lima, J.R. Keys, B.C. Blaxall, J.A. Petrofski, A. Jakoi, C.A. Milano, W.J. Koch, Lymphocyte levels of GRK2 (betaARK1) mirror changes in the LVAD-supported failing human heart: lower GRK2 associated with improved beta-adrenergic signaling after mechanical unloading, J. Card. Fail. 12 (2006) 360–368.
[22] R.E. Bonita, P.W. Raake, N.J. Otis, J.K. Chuprun, T. Spivack, A. Dasgupta, D.J. Whellan, P.J. Mather, W.J. Koch, Dynamic changes in lymphocyte GRK2 levels in cardiac transplant patients: a biomarker for left ventricular function, Clin. Transl. Sci. 3 (2010) 14–18.
[23] R.J. Lefkowitz, G protein-coupled receptors and receptor kinases: from molecular biology to potential therapeutic applications, Nat. Biotechnol. 14 (1996) 283–286.
[24] (a) G. Iaccarino, W.J. Koch, Therapeutic potential of G-protein coupled receptor kinases in the heart, Expert Opin. Investig. Drugs 8 (1999) 545–554;
(b) G. Rengo, A. Lymperopoulos, D. Leosco, W.J. Koch, GRK2 as a novel gene therapy target in heart failure, J. Mol. Cell Cardiol. 50 (2011) 785–792.
[25] H.A. Rockman, K.R. Chien, D.J. Choi, G. Iaccarino, J.J. Hunter, J. Ross Jr., R.J. Lefkowitz, W.J. Koch, Expression of a beta-adrenergic receptor kinase 1 inhibitor prevents the development of myocardial failure in gene-targeted mice, Proc. Natl. Acad. Sci. U. S. A. 95 (1998) 7000–7005.
[26] J. Setyawan, K. Koide, T.C. Diller, M.E. Bunnage, S. Taylor, K.C. Nicolai, L.L. Brunton, Inhibition of protein kinases by balanol: specificity within the serina/threonina protein kinase subfamily, Mol. Pharmacol. 56 (1999) 370–376.

[27] M. Iino, T. Furugori, T. Mori, S. Moriyama, A. Fukuzawa, T. Shibano, Rational design and evaluation of new lead compounds for selective βARK1 inhibitors, J. Med. Chem. 45 (2002) 2150–2159.
[28] J.L. Benovic, W.C. Stone, M.G. Caron, R.J. Lefkowitz, Inhibition of the β-adrenergic receptor kinase by polyanions, J. Biol. Chem. 264 (1989) 6707–6710.
[29] Takeda Pharmaceuticals Company Limited, S. Ikeda, M. Kaneko, S. Fujiwara, Cardiotonic Agents Comprising GRK Inhibitor, World Patent WO2007034846.
[30] R. Winstel, H.G. Ihlenfeldt, G. Jung, C.M.J. Krasel, Lohse, Peptide inhibitors of G protein-coupled receptor kinases, Biochem. Pharmacol. 70 (2005) 1001–1008.
[31] M.Y. Niv, H. Rubin, J. Cohen, L. Tsirulnikov, T. Licht, A. Peretzman-Shemer, E. Cna'an, A. Tartakovsky, I. Stein, S. Albeck, I. Weinstein, M. Goldenberg-Furmanov, D. Tobi, E. Cohen, M. Laster, S.A. Ben-Sasson, H. Reuveni, Sequence-based design of kinase inhibitors applicable for therapeutics and target identification, J. Biol. Chem. 279 (2004) 1242–1255.
[32] Y. Anis, O. Leshem, H. Reuveni, I. Wexler, R. Ben Sasson, B. Yahalom, M. Laster, I. Raz, S. Ben Sasson, E. Shafrir, E. Ziv, Antidiabetic effect of novel modulating peptides of G-protein-coupled kinase in experimental models of diabetes, Diabetologia 47 (2004) 1232–1244.
[33] G. Mayer, B. Wulffen, C. Huber, J. Brockmann, B. Flicke, L. Neumann, D. Hafenbradl, B.M. Kleb, M.J. Lohse, C. Krasel, M. Blind, An RNA molecule that specifically inhibits G-protein coupled receptor kinase 2 in vitro, RNA 14 (2008) 524–534.
[34] E. Cipolletta, A. Campanile, G. Santulli, E. Sanzari, D. Leosco, P. Campiglia, B. Trimarco, G. Iaccarino, The G protein coupled receptor kinase 2 plays an essential role in beta-adrenergic receptor-induced insulin resistance, Cardiovasc. Res. 84 (2009) 407–415.
[35] I. Gomez-Monterrey, A. Carotenuto, E. Cipolletta, M. Sala, E. Vernieri, A. Limatola, A. Bertamino, S. Musella, P. Grieco, B. Trimarco, E. Novellino, G. Iaccarino, P. Campiglia, SAR study and conformational analysis of a series of novel peptide G protein-coupled receptor kinase 2 (GRK2) inhibitors, Biopolymers (2013), http://dx.doi.org/10.1002/bip.22295.
[36] J.J.G. Tesmer, V.M. Tesmer, T. David, D.T. Lodowski, H. Steinhagen, J. Huber, Structure of human G protein-coupled receptor kinase 2 in complex with the kinase inhibitor balanol, J. Med. Chem. 53 (2010) 1867–1870.
[37] E. Atherton, R.C. Sheppard, Solid-phase Peptide Synthesis: A Practical Approach, IRL Press, Oxford, UK, 1989.
[38] X. Chen, R. Park, A.H. Shahinian, J.R. Bading, P.S. Conti, Pharmacokinetics and tumor retention of 125I-labeled RGD peptide are improved by PEGylation, Nucl. Med. Biol. 31 (2004) 11–19.
[39] P. Grieco, P.M. Gitu, V.J. Hruby, Preparation of 'side-chain-to-side-chain' cyclic peptides by allyl and alloc strategy: potential for library synthesis, J. Pept. Res. 57 (2001) 250–256.
[40] K. Wüthrich, NMR of Proteins and Nucleic Acids, Wiley-Interscience, 1986.
[41] D.S. Wishart, B.D. Sykes, F.M. Richards, The Chemical Shift Index: a fast method for the assignment of protein secondary structure through NMR spectroscopy, Biochemistry 31 (1992) 1647–1651.
[42] P. Güntert, C. Mumenthaler, K. Wüthrich, Torsion angle dynamics for NMR structure calculation with the new program DYANA, J. Mol. Biol. 273 (1997) 283–298.
[43] C. Gilon, C. Mang, E. Lohof, A. Friedler, H. Kessler, Synthesis of Peptides and Peptidomimetics, Georg Thieme Verlag Eds, Stuggart, 2003.
[44] (a) B. Hargittai, N.A. Solé, D.R. Groebe, S.N. Abramson, G. Barany, Chemical syntheses and biological activities of lactam analogues of alpha-conotoxin SI, J. Med. Chem. 43 (2000) 4787–4792;
(b) P. Grieco, A. Carotenuto, R. Patacchini, C.A. Maggi, E. Novellino, P. Rovero, Design, synthesis, conformational analysis, and biological studies of urotensin-II lactam analogues, Bioorg. Med. Chem. 10 (2002) 3731–3739.
[45] G. Iaccarino, E. Barbato, E. Cipolletta, A. Esposito, A. Fiorillo, W.J. Koch, B. Trimarco, Cardiac betaARK1 upregulation induced by chronic salt deprivation in rats, Hypertension 38 (2001) 255–260.
[46] A. Perino, A. Ghigo, E. Ferrero, F. Morello, G. Santulli, G.S. Baillie, F. Damilano, A.J. Dunlop, C. Pawson, R. Walser, R. Levi, F. Altruda, L. Silengo, L.K. Langeberg, G. Neubauer, S. Heymans, G. Lembo, M.P. Wymann, R. Wetzker, M.D. Houslay, G. Iaccarino, J.D. Scott, E. Hirsch, Integrating cardiac PIP3 and cAMP signaling through a PKA anchoring function of p110γ, Mol. Cell 42 (2011) 84–95.
[47] (a) K. Shiraki, K. Nishikawa, Y. Goto, Trifluoroethanol-induced stabilization of the alpha-helical structure of beta-lactoglobulin: implication for non-hierarchical protein folding, J. Mol. Biol. 254 (1995) 180–194;
(b) I. Gomez-Monterrey, M. Sala, M.R. Rusciano, S. Monaco, A.S. Maione, G. Iaccarino, P. Tortorella, A.M. D'Ursi, M. Scrima, A. Carotenuto, G. De Rosa, A. Bertamino, E. Vernieri, P. Grieco, E. Novellino, M. Illario, P. Campiglia, Characterization of a selective CaMKII peptide inhibitor, Eur. J. Med. Chem. 62 (2013) 425–434;
(c) A. Carotenuto, M.C. Alcaro, M.R. Saviello, E. Peroni, F. Nuti, A.M. Papini, E. Novellino, P. Rovero, Designed glycopeptides with different β-turn types as synthetic probes for the detection of autoantibodies as biomarkers of multiple sclerosis, J. Med. Chem. 51 (2008) 5304–5309.
[48] (a) A. Di Cianni, A. Carotenuto, D. Brancaccio, E. Novellino, J.C. Reubi, K. Beetschen, A.M. Papini, M. Ginanneschi, Novel octreotide dicarba-analogues with high affinity and different selectivity for somatostatin receptors, J. Med. Chem. 53 (2010) 6188–6197;
(b) P. Grieco, A. Carotenuto, L. Auriemma, M.R. Saviello, P. Campiglia, I. Gomez-Monterrey, L. Marcellini, V. Luca, D. Barra, E. Novellino, M.L. Mangoni, The effect of D-amino acids substitution on the selectivity of temporin L towards target cells: identification of a potent anti-Candida peptide, Biochim. Biophys. Acta 1828 (2013) 652–660.
[49] T.L. Hwang, A. Shaka, Water suppression that works. Excitation sculpting using arbitrary wave-forms and pulsed-field gradients, J. Magn. Reson. 112 (1995) 275–279.
[50] U. Piantini, O.W. Sorensen, R.R. Ernst, Multiple quantum filters for elucidating NMR coupling networks, J. Am. Chem. Soc. 104 (1982) 6800–6801.
[51] L. Braunschweiler, R.R. Ernst, Coherence transfer by isotropic mixing: application to proton correlation spectroscopy, J. Magn. Reson. 53 (1983) 521–528.
[52] J. Jeener, B.H. Meier, P. Bachman, R.R. Ernst, Investigation of exchange processes by two-dimensional NMR spectroscopy, J. Chem. Phys. 71 (1979) 4546–4553.
[53] D.J. States, R.A. Haberkorn, D.J. Ruben, A two-dimensional nuclear Overhauser experiment with pure absorption phase in four quadrants, J. Magn. Reson. 48 (1982) 286–292.
[54] C. Bartels, T. Xia, M. Billeter, P. Güntert, K. Wüthrich, The program XEASY for computer-supported NMR spectral analysis of biological macromolecules, J. Biomol. NMR 6 (1995) 1–10.
[55] J.R. Maple, U. Dinur, A.T. Hagler, Derivation of force fields for molecular mechanics and dynamics from ab initio energy surfaces, Proc. Natl. Acad. Sci. U. S. A. 85 (1988) 5350–5354.
[56] E.F. Pettersen, T.D. Goddard, C.C. Huang, G.S. Couch, D.M. Greenblatt, E.C. Meng, T.E. Ferrin, Ucsf Chimera-a visualization system for exploratory research and analysis, J. Comput. Chem. 25 (2004) 1605–1612.
[57] R. Koradi, M. Billeter, K. Wüthrich, MOLMOL: a program for display and analysis of macromolecular structures, J. Mol. Graph 14 (1996) 51–55.
[58] M.-C. Cho, M. Rao, W.J. Koch, S.A. Thomas, R.,D. Palmiter, H.A. Rockman, Enhanced contractility and decreased β-adrenergic receptor kinase-1 in mice lacking endogenous norepinephrine and epinephrine, Circulation 99 (1999) 2702–2707.